The 300 and 0 K volume susceptibilities as corrected for core diamagnetism are shown in Table III. Figure 10 shows the values plotted as functions of composition together with corresponding values of T_c. It is remarkable that both χ_v(0 K) and T_c exhibit the same composition dependence.

Pauli susceptibility, in general, is intimately related to the band structure of a compound. In the presence of complicated structure in the band, the 0 K Pauli volume susceptibility would be proportional to the density states at the Fermi level $N(\epsilon_F)$. Figure 10 indicates that T_c in these compounds depends strongly on $N(\epsilon_F)$, as would be in qualitative agreement with the simple BCS theory prediction (eq 3).

$$T_c \approx \langle\omega\rangle \exp[-1/(N(\epsilon_F))V] \quad (3)$$

The fact that T_c and $N(\epsilon_F)$ are similarly dependent on c/a is puzzling. No immediate connection between c/a and $N(\epsilon_F)$ is apparent. Overlap between unit cells should depend on a_H alone, as is evident from $SnMo_6S_{8-x}$.[8] More detailed band-structure calculations are needed to elucidate the relationship of T_c, c/a, and the susceptibility.

By way of summary, we have presented evidence for ordering of chalcogens in $PbMo_6(S_{1-x}Se_x)_8$ with respect to general- and special-position sites. The superconducting transition temperatures were found to be a linear function of c/a until selenium atoms substantially occupy the special-position sites. The 0 K volume susceptibility exhibits the same composition dependence as T_c, suggesting variations in T_c reflect changes in the density of states at the Fermi level. The manner in which c/a and $N(\epsilon_F)$ are connected is unclear; it needs to be investigated in more detail.

Registry No. $PbMo_6S_8$, 39432-49-0; $PbMo_6Se_8$, 62462-65-1.

Contribution from the Institute of Inorganic and Analytical Chemistry and the Institute of Crystallography, University of Lausanne, CH-1005 Lausanne, Switzerland

Study of $PtX_2(PR_3)_2$ in the Presence of PR_3 in CH_2Cl_2 Solution and the Cis-Trans Isomerization Reaction As Studied by ^{31}P NMR. Crystal Structure of $[PtCl(PMe_3)_3]Cl$

ROLAND FAVEZ,[1a,b] RAYMOND ROULET,*[1a] ALAN A. PINKERTON,[1c] and DIETER SCHWARZENBACH[1c]

Received May 18, 1979

The identity of the species present in dichloromethane solutions of PtX_2L_2 and L (L = PMe_3, PEt_3, P-*n*-Bu_3, $P(tol)_3$ where tol = *p*-tolyl; Pt:L ratios from 1:0.05 to 1:5) are *cis*- and *trans*-PtX_2L_2, $[PtXL_3]^+$ (X = Cl, Br), and $[PtXL_4]^+$ (X = Cl, Br, I; L = PMe_3). The only species with three coordinated phosphines which is five-coordinate in solution is $PtI_2(PMe_3)_3$, whose IR and NMR parameters are consistent with a square-pyramidal geometry having one phosphine in the apical position. All other "tris" complexes $[PtXL_3]^+$ are four-coordinate in solution as shown by UV and ^{31}P NMR spectroscopy, and this geometry is also found in the solid state ($[PtCl(PMe_3)_3]Cl$ X-ray crystal structure). The complexes $[PtX(PMe_3)_4]^+$ have a square-pyramidal geometry with X in the apical position. In the case of L = PMe_3, ^{31}P NMR studies show that intermolecular phosphine exchange occurs between $[PtClL_3]^+$, $[PtClL_4]^+$, PtI_2L_3, and free L, whose activation parameters, estimated from line-shape analysis, are reported. Contrary to previous reports, chloride ion is found to displace one phosphine from $[PtClL_3]^+$ ion, giving the *cis*-$PtCl_2L_2$ isomer in a fast step prior to cis-trans equilibration. The results indicate that the cis-trans isomerization of PtX_2L_2 catalyzed by L proceeds by rapid displacement of X^- by L followed by slow displacement of L by X^- and not by pseudorotation of a five-coordinate intermediate. A similar mechanism was established for the isomerization of the alkyl complex $PtCl(CH_2CN)(PPh_3)_2$.

Introduction

Since the original proposal by Basolo and Pearson[2] of the double displacement mechanism for the phosphine-catalyzed cis-trans isomerization of tetragonal-planar platinum(II) complexes, many studies[3-18] with conflicting results and interpretations[3-6,15] have appeared in the literature. The following mechanisms have been proposed to date: (a) a double displacement mechanism (eq 1) which implies phosphine exchange and an ionic intermediate from which X^- is able to displace L (This mechanism is in agreement with the stereospecific nature of all substitution reactions of platinum(II) complexes observed so far.), (b) a pseudorotation mechanism

$$cis\text{-}PtX_2L_2 + L \underset{\text{fast}}{\rightleftharpoons} [PtXL_3]^+ + X^- \underset{\text{slow}}{\rightleftharpoons} trans\text{-}PtX_2L_2 + L \quad (1)$$

(1) (a) Institut de Chimie Minérale et Analytique. (b) Based, in part, on the Ph.D. thesis of R.F., Université de Lausanne. (c) Institut de Cristallographie.
(2) Basolo, F.; Pearson, R. G. "Mechanisms of Inorganic Reactions", 2nd ed.; Wiley: New York, 1967; p 424.
(3) Haake, P; Pfeiffer, R. M. *J. Am. Chem. Soc.* **1970**, *92*, 4996.
(4) Haake, P.; Pfeiffer, R. M. *Chem. Commun.* **1969**, 1330; *J. Am. Chem. Soc.* **1970**, *92*, 5243.
(5) Cooper, D. G.; Powell, J. *J. Am. Chem. Soc.* **1973**, *95*, 1102.
(6) Cooper, D. G.; Powell, J. *Can. J. Chem.* **1973**, *51*, 1634.
(7) Louw, W. J. *J. Chem. Soc., Chem. Commun.* **1974**, 353.
(8) Powell, J; Cooper, D. G. *J. Chem. Soc., Chem. Commun.* **1974**, 749.
(9) Redfield, D. A.; Nelson, J. H. *J. Am. Chem.* Soc. **1974**, *96*, 6219.
(10) Redfield, D. A.; Nelson, J. H. *Inorg. Chem.* **1973**, *12*, 15. Verstuyft, A. W.; Nelson, J. H. *Ibid.* **1975**, *14*, 1501.
(11) Redfield, D. A.; Nelson, J. H.; Henry, R. A; Moore, D. W.; Jonassen, H. B. *J. Am. Chem. Soc.* **1974**, *96*, 6298.
(12) Redfield, D. A.; Cary, L. W.; Nelson, J. H. *Inorg. Chem.* **1975**, *14*, 50.
(13) Verstuyft, A. W.; Cary, L. W.; Nelson, J. H. *Inorg. Chem.* **1976**, *15*, 3161.
(14) Pfeiffer, R. M. *Synth. React. Inorg. Met.-Org. Chem.* **1976**, *6*, 55.
(15) Louw, W. J. *Inorg. Chem.* **1977**, *16*, 2147.
(16) Faraone, G.; Ricevuto, U.; Romeo, R.; Trozzi, M. *J. Chem. Soc. A* **1971**, 1877.
(17) Romeo, R.; Minniti, D.; Trozzi, M. *Inorg. Chim. Acta* **1975**, *14*, L15; *Inorg. Chem.* **1976**, *15*, 1134. Romeo, R. *Ibid.* **1978**, *17*, 2040.
(18) Jensen, K. A. *Z. Anorg. Allg. Chem.* **1936**, *229*, 225.

0020-1669/80/1319-1356$01.00/0

(eq 2) proposed by Haake et al.[3] which implies a five-coor-

$$cis\text{-}PtX_2L_2 + L' \rightleftarrows PtX_2L_2L' \rightleftarrows trans\text{-}PtX_2L_2 + L' \quad (2)$$

dinate transition state or intermediate (PtX_2L_2L' must be able to undergo a fluxional change which interconverts the position of L and X but not L and L' during isomerization.), (c) the consecutive displacement of a neutral ligand by a neutral ligand (eq 3) proposed by Redfield and Nelson[9] where A and

$$cis\text{-}PtX_2L_2 + L' \rightleftarrows PtX_2L_2L' \text{ (A)} \rightleftarrows PtX_2LL' + L \rightleftarrows PtX_2L'L_2 \text{ (B)} \rightleftarrows trans\text{-}PtX_2L_2 + L' \quad (3)$$

B may be either transition states or intermediates and are not necessarily identical (These authors showed that there is phosphine mixing in these systems and that PtX_2LL' can be isolated in certain cases. They suggested that mechanism a should dominate in polar solvents when X^- is poorly coordinating and L' is a strong base, pathway b in nonpolar solvents when L and L' have nearly the same basicity and are small, and pathway c in nonpolar solvents when X^- is strongly coordinating.), (d) a dissociative mechanism (eq 4) proposed by

$$cis\text{-}PtXRL_2 \rightleftarrows [PtRL_2]^+ + X^- \rightleftarrows trans\text{-}PtXRL_2 \quad (4)$$

Romeo et al.[16] for the spontaneous isomerization of aryl- and alkylplatinum(II) complexes, which implies a dissociative step generating a 14-electron species.[17]

Arguments derived from the rate dependence on [L] are useless since pathways a, b, and c will obey the same second-order rate law. Kinetic measurements with $L \neq L'$ are difficult to interpret since the thermodynamic stability of the mixed-species PtX_2LL' must be taken into account. ^1H NMR spectroscopy is helpful, but temperature-dependent spectra for most of these tertiary phosphine systems are superimposed non-first-order patterns intractable by line-shape analysis; e.g., see the conflicting discussions on the system $PtX_2(PPhMe_2)_2 + PPhMe_2$.[5,15] Experimental investigation should concentrate on the characterization of intermediates in solution by the most direct method. For this reason, we have used ^{31}P NMR spectroscopy to examine the systems $PtX_2L_2 + L$ (L = PMe_3, PEt_3, P-*n*-Bu_3, P(tol)$_3$ where tol = *p*-tolyl) and report our results herein, as well as the crystal structure of $[PtCl(PMe_3)_3]Cl$.

Results and Discussion

1. Studies of PtX_2L_2 and L in Dichloromethane Solution (L = PMe_3, PEt_3, P-*n*-Bu_3, P(tol)$_3$). Identification of the Species Present. The synthesis[18,19] and spectral properties of *cis*- and *trans*-PtX_2L_2 are well established (X = halide; L = PMe_3,[20-22] PEt_3,[20-23,24] P-*n*-Bu_3[25,26]). Cis-trans thermal isomerization occurs in solution when a trace of L is added and the equilibrium thermodynamic parameters have been determined in benzene (L = PEt_3,[27] P-*n*-Pr_3, P-*n*-Bu_3[28]). Similar experiments have been carried out in various solvents for the palladium analogues PdX_2L_2 (L = PPh_2Me, $PPhMe_2$; X = Cl,[29] N_3[30]). Complexes with three bonded phosphines have been isolated in the solid state and formulated as four-coordinate ionic species, $[PtXL_3]^+$ (L = PMe_3,[19] PEt_3, P-*n*-Bu_3[31]), or as five-coordinate neutral PtX_2L_3 (L = 2-phenylphosphindoline;[32] L = $PPhMe_2$; X = Br, I).[33] However no crystal structure determination of these "tris" complexes has been reported to date. Complexes with four (but none with five) bonded phosphines have been isolated in the solid state, e.g., $[Pt(PMe_3)_4](BF_4)_2$,[20] and these "tetrakis" species in solution were invariably formulated as four-coordinate $[PtL_4]^{2+}$ ions, except for $[PtH(PEt_3)_4]^+$[34] and $[Pt(alkyl)(PPhMe_2)_4]^+$.[35] As the rate of cis–trans isomerization of PtX_2L_2 (X = halide) is first order in both the complex and L, a knowledge of the geometry and dynamic properties of species having more than two bonded phosphines is crucial to a discussion of the isom-

Table I. The System $PtX_2(PMe_3)_2$ and PMe_3 in CH_2Cl_2 Solution

starting complex	$[PMe_3]_{added}/[Pt]$	species in soln
trans-$PtX_2(PMe_3)_2$ (X = Cl, Br)	trace[b]	*cis*-$PtX_2(PMe_3)_2$ (>99%)
cis-$PtI_2(PMe_3)_2$	trace[b]	*trans*-$PtI_2(PMe_3)_2$ (>99%)
$PtX_2(PMe_3)_2$ (X = Cl, Br)[a]	0.5[c]	*cis*-$PtX_2(PMe_3)_2$ + $[PtX(PMe_3)_3]^+$ (1:1)
	1.0[c]	$[PtX(PMe_3)_3]^+$ (>99%)
	1.5[d]	$[PtX(PMe_3)_3]^+$ + $[PtX(PMe_3)_4]^+$ (1:1)
	2.0[d]	$[PtX(PMe_3)_4]^+$ (>99%)
	10[d]	$[PtX(PMe_3)_4]^+$ + PMe_3 (1:8)
$PtI_2(PMe_3)_2$[a]	0.5[c]	*trans*-$PtI_2(PMe_3)_2$ + $PtI_2(PMe_3)_3$ (1:1)
	1.0[c]	$PtI_2(PMe_3)_3$ (>99%)
	1.5[d]	$PtI_2(PMe_3)_3$ + $[PtI(PMe_3)_4]^+$ (1:1)
	2.0[d]	$[PtI(PMe_3)_4]^+$ (>99%)
	5.0[e]	$[PtI(PMe_3)_4]^+$ + PMe_3 (1:3)

[a] Cis or trans. [b] At 30 °C. [c] At −40 °C. [d] At −65 °C. [e] In $CHClF_2$ at −155 °C.

Table II. The System $PtCl_2L_2$ and L in CH_2Cl_2 Solution (L = PEt_3, P-*n*-Bu_3, P(tol)$_3$)

starting complex	$[L]_{added}/[Pt]$	species in soln at 30 °C
	L = PEt_3	
cis- or *trans*-$PtCl_2L_2$	trace	*cis*- + *trans*-$PtCl_2L_2$ (0.90:0.10)
trans-$PtCl_2L_2$ + $AgBF_4$ (1:0.80)	1.0	$[PtClL_3]^+$ + *trans*-$PtCl_2L_2$ (0.8:0.2)[a]
cis- or *trans*-$PtCl_2L_2$	3.0	$[PtClL_3]^+$ + L (1:2)
	L = P-*n*-Bu_3	
cis- or *trans*-$PtCl_2L_2$	trace	*cis*- + *trans*-$PtCl_2L_2$ (0.92:0.08)
trans-$PtCl_2L_2$	1.0	$[PtClL_3]^+$ + *cis*- + *trans*-$PtCl_2L_2$ + L (0.15:0.80:0.05:0.85)
trans-$PtCl_2L_2$	3.0	$[PtClL_3]^+$ + L (1:2)
	L = P(tol)$_3$	
cis- or *trans*-$PtCl_2L_2$	trace	*cis*- + *trans*-$PtCl_2L_2$ (0.84:0.16)
trans-$PtCl_2L_2$ + $AgNO_3$ (1:1)	1.0	$[PtClL_3]^+$ + $[Pt(NO_3)L_3]^+$ (1:1)
trans-$PtCl_2L_2$	2.67	$[PtClL_3]^+$ + *cis*- + *trans*-$PtCl_2L_2$ + L (0.20:0.84:0.16:3.00)

[a] Species present prior to cis–trans equilibration.

(19) Hartley, F. R. *Organomet. Chem. Rev.* **1970**, *6*, 126.
(20) Duddell, D. A.; Goggin, P. L.; Goodfellow, R. J.; Norton, M. G.; Smith, J. G. *J. Chem. Soc. A* **1970**, 545.
(21) Duddell, D. A.; Evans, J. G.; Goggin, P. L.; Goodfellow, R. J.; Rest, A. J.; Smith, J. G. *J. Chem. Soc. A* **1969**, 2134.
(22) Goggin, P. L; Goodfellow, R. J.; Haddock, S. R.; Knight, J. R.; Reed, F. J. S.; Taylor, B. F. *J. Chem. Soc., Dalton Trans.* **1974**, 523.
(23) Grimm, S. O.; Keiter, R. L.; McFarlane, W. *Inorg. Chem.* **1967**, *6*, 1133.
(24) Pregosin, P. S.; Sze, Siu Ning. *Helv. Chim. Acta* **1978**, *61*, 1878.
(25) *Inorg. Synth.* **1963**, *7*, 245.
(26) Pidcock, A.; Richards, R. E.; Venanzi, L. M. *J. Chem. Soc. A* **1966**, 1707.
(27) Chatt, J.; Wilkins, R. G. *J. Chem. Soc.* **1952**, 273.
(28) Chatt, J.; Wilkins, R. G. *J. Chem. Soc.* **1956**, 525.
(29) Redfield, D. A.; Nelson, J. H. *Inorg. Chem.* **1973**, *12*, 15.
(30) Redfield, D. A.; Cary, L. W.; Nelson, J. H. *Inorg. Chem.* **1975**, *14*, 50.
(31) Church, M. J.; Mays, M. J. *J. Chem. Soc. A* **1968**, 3074.
(32) Collier, J. W.; Mann, F. G.; Watson, D. G.; Watson, H. R. *J. Chem. Soc.* **1964**, 1803.
(33) Pearson, R. G.; Louw, W.; Rajaram, J. *Inorg. Chim. Acta* **1974**, *9*, 251.
(34) English, A. D.; Meakin, P.; Jesson, J. P. *J. Am. Chem. Soc.* **1976**, *98*, 422.
(35) Favez, R. Thèse de doctorat, Université de Lausanne, 1979.
(36) Goggin, P. L.; Goodfellow, R. J.; Knight, J. R.; Norton, M. G.; Taylor, B. F. *J. Chem. Soc., Dalton Trans.* **1973**, 2220.
(37) Mather, G. G.; Pidcock, A.; Rapsey, G. J. N. *J. Chem. Soc., Dalton Trans.* **1973**, 2095.

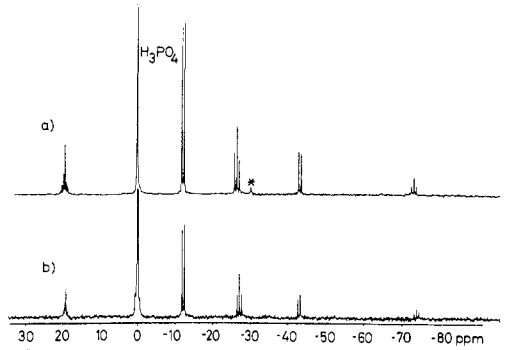

Figure 1. $^{31}P\{^1H\}$ FT NMR spectra in CD_2Cl_2 at −40 °C of (a) a mixture of *cis*-$PtCl_2(PMe_3)_2$ and PMe_3 (1:1.05) and (b) $[PtCl(PMe_3)_3]ClO_4$ (asterisk: $[PtCl(PMe_3)_4]^+$).

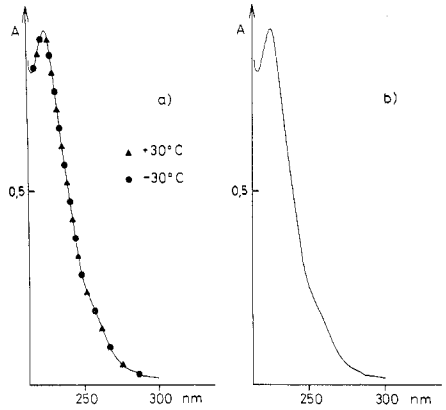

Figure 2. UV spectra in dichloromethane of (a) $[PtCl(PMe_3)_3]Cl$ at −30 and +30 °C and (b) $[PtCl(PMe_3)_3]ClO_4$ ($[Pt] = 1.01 \times 10^{-4}$ M).

erization mechanism. We have thus prepared a series of solutions of PtX_2L_2 and L and compared their $^{31}P\{^1H\}$ FT NMR spectra with those of known PtX_2L_2, $[PtXL_3]^+$, and $[PtL_4]^{2+}$ complexes. The identity of the species present in dichloromethane solution is given in Table I for L = PMe_3 and in Table II for L = PEt_3, P-*n*-Bu_3, P(tol)$_3$. On the NMR time scale, intermolecular exchange at room temperature between PtX_2L_2 and L (L = PMe_3, PEt_3, P-*n*-Bu_3, P(tol)$_3$) and $[PtXL_3]^+$ and L (L = PEt_3, P-*n*-Bu_3, P(tol)$_3$) is slow, but in the case of $[PtX(PMe_3)_3]^+$, $[PtX(PMe_3)_4]^+$, or $PtI_2(PMe_3)_3$ and free PMe_3, a fast exchange is observed. In the latter case, the ^{31}P NMR spectra were recorded at the low-temperature slow-exchange limit, and the spectral data of all observed species are summarized in Table III.

In all cases but one (L = PMe_3; X = I), the "tris" species in solution are formulated as four-coordinate $[PtXL_3]^+$ for the following reasons: (i) the ^{31}P NMR spectrum of PtX_2L_2 + L (1:1) is identical with that of $[PtXL_3]Y$ (Y = ClO_4 or PF_6; e.g., Figure 1); (ii) the UV spectra of PtX_2L_2 + L (1:1) and of some isolated $[PtXL_3]X$ are identical with those of the corresponding $[PtXL_3]Y$ (e.g., Figure 2); (iii) the IR spectrum of $[PtClL_3]Cl$ presents only one ν(Pt–Cl) band in the solid state and in solution; (iv) there is no ^{35}Cl NMR evidence of contact ion pairing in CD_2Cl_2. The ^{35}Cl NMR spectrum of $[PtCl(PMe_3)_3]ClO_4$ at room temperature presents a single resonance attributable to the perchlorate anion whose width at half-height (4 Hz) is close to that of $NaClO_4$ in D_2O (3 Hz). Stengle and Berman[38] have shown that the formation of contact ion pairs broadens this resonance by a factor $\sim 10^2$. For L = PMe_3, the fast phosphine exchange precluded the observation of the characteristic ^{31}P NMR pattern of $[PtXL_3]^+$ at room temperature (a doublet and a triplet, intensity ratio 2:1). However, the UV spectrum did not change between −30 and +30 °C (Figure 2). Thus, even for this system, no evidence was found for the hypothetical $PtCl_2L_3$ in dichloromethane solution. An X-ray diffraction study of $[PtCl(PMe_3)_3]Cl$ showed that this compound is also a four-coordinate complex in the solid state (vide infra).

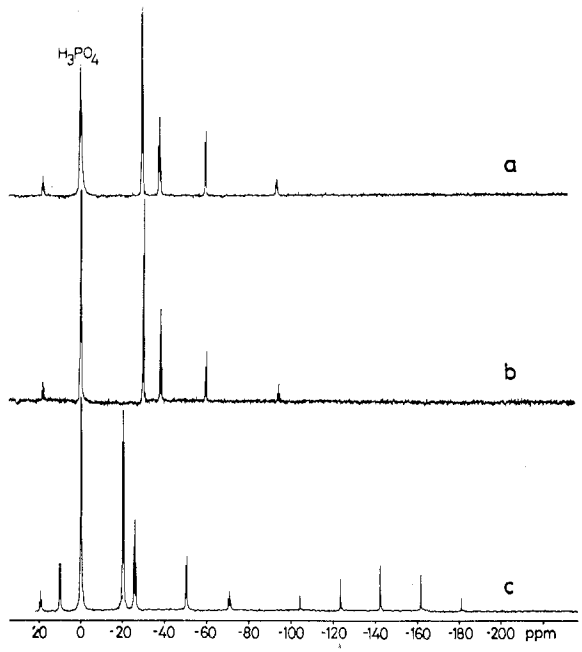

Figure 3. $^{31}P\{^1H\}$ FT NMR spectra in CD_2Cl_2 at −40 °C of (a) a mixture of *trans*-$PtI_2(PMe_3)_2$ and PMe_3 (1:1), (b) $PtI_2(PMe_3)_3$, and (c) $[PtI(PMe_3)_3]PF_6$.

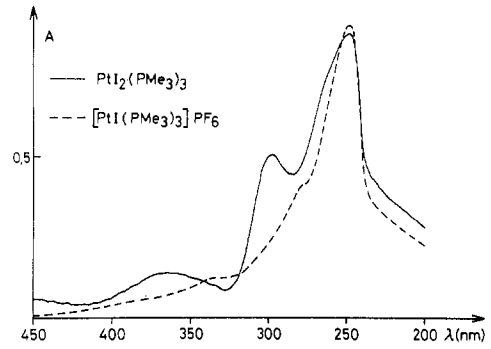

Figure 4. UV spectra in dichloromethane of (a) $PtI_2(PMe_3)_3$ and (b) $[PtI(PMe_3)_3]PF_6$, [Pt] = 2.58×10^{-5} M.

By contrast, $PtI_2(PMe_3)_3$ is a five-coordinate complex in dichloromethane solution (crystals of this compound suitable for X-ray diffraction could unfortunately not be obtained). Its ^{31}P NMR and UV spectra are identical with those of a mixture of *trans*-$PtI_2(PMe_3)_2$ and PMe_3 (1:1) but are different from those of $[PtI(PMe_3)_3]PF_6$ (Figures 3 and 4). The ^{31}P doublet and triplet are shifted to high field, and one ^1J(Pt,P) coupling constant is quite uncharacteristic of a phosphorus atom in a trans position to iodide ion in a "square-planar" environment. The NMR pattern may arise from various ideal geometries: a trigonal bipyramid with (i) one PMe_3 and (ii) two PMe_3 in axial positions or a square pyramid with (iii) one iodide ion in the apical position, (iv) one PMe_3 in the apical position and two basal iodide ions in cis positions to each other, and (v) one PMe_3 in the apical position and two basal iodide ions trans to each other. Meakin and Jesson[39] have shown in

(38) Berman, H. A.; Stengle, T. R. *J. Phys. Chem.* **1975**, *79*, 1001.

(39) Meakin, P.; Jesson, J. P. *J. Am. Chem. Soc.* **1974**, *96*, 5751.

Table III. ^{31}P NMR Parameters for Tertiary Phosphine Complexes of Platinum(II)

		trans to X		trans to P			
no.	complex	$\delta(P_1)$	$^1J(P_1, Pt)$	$\delta(P_2)$	$^1J(P_2, Pt)$	$^2J(P, P)$	ref
1a,b	*cis*- and *trans*-$PtCl_2(PMe_3)_2$	−24.9	3489	−15.8	2386		*a*
		−24	3480	−15.8	2379		22[b]
2a,b	*cis*- and *trans*-$PtBr_2(PMe_3)_2$	−25.1	3439	−21.5	2324		*a*
		−23.8	3426	−20.4	2336		22[b]
3a,b	*cis*- and *trans*-$PtI_2(PMe_3)_2$	−27.3	3317	−32.3	2236		*a*
		−26.0	3306	−32.2	2230		22[b]
4	$[PtCl(PMe_3)_3]ClO_4$	−26.9	3370	−12.0	2231	22	*a*
		−27.5	3402	−12.6	2266	23	36[b,c]
5	$[PtCl(PMe_3)_3]Cl$	−26.8	3368	−12.0	2230	22	*a*
6	$[PtBr(PMe_3)_3]PF_6$[d]	−25.5	3406	−15.6	2233	22	*a*
		−25.6	3412	−16.6	2255	25	36[b,c]
7	$[PtBr(PMe_3)_3]Br$	−25.5	3404	−15.6	2231	24	*a*
8	$[PtI(PMe_3)_3]PF_6$[d]	−26.1	3329	−20.3	2227	21	*a*
		−26.1	3349	−20.5	2248	27	36[b,c]
9	$PtI_2(PMe_3)_3$	−38.2	4082	−30.3	2164	20	*a*
10	$[PtCl(PMe_3)_4]Cl$	...	...	−30.1	2465		*a*
11	$[PtBr(PMe_3)_4]Br$	...	...	−31.8	2497		*a*
12	$[PtI(PMe_3)_4]I$	...	...	−35.4	2420		*a*
13	$[Pt(PMe_3)_4](BF_4)_2$	...	...	−21.5	2230		35[b]
14a,b	*cis*- and *trans*-$PtCl_2(PEt_3)_2$	9.0	3502	12.1	2394		*a*
		9.3	3518	12.2	2397		24
15	$[PtCl(PEt_3)_3]ClO_4$	9.9	3442	17.6	2263	19	*a*
			3499		2233		37
16	$[PtCl(PEt_3)_3]Cl$	9.8	3446	17.4	2266	19	*a*
17a,b	*cis*- and *trans*-$PtCl_2(P\text{-}n\text{-}Bu_3)_2$	0.9	3505	4.5	2379		*a*
		1.4	3508	4.9	2380		26[e]
18	$[PtCl(P\text{-}n\text{-}Bu_3)_3]ClO_4$	1.4	3441	10.2	2267	19	*a*
			3459		2266		37
19	$[PtCl(P\text{-}n\text{-}Bu_3)_3]Cl$	1.3	3440	10.0	2264	19	*a*
20a,b	*cis*- and *trans*-$PtCl_2(P(tol)_3)_2$	12.2	3694	18.4	2595		*a*
21	$[PtCl(P(tol)_3)_3]ClO_4$	18.7	3645	29.8	2475	18	*a*
22	$[PtCl(P(tol)_3)_3]Cl$	18.9	3641	29.6	2470	18	*a*
23	$[PtNO_3(P(tol)_3)_3]Cl$	−0.7	3783	19.9	2600	19	*a, f*

[a] This work; in CD_2Cl_2 at −40 °C for **4–9**, at −50 °C for **10–12**, and at room temperature for all other complexes. Chemical shifts are in ppm referred to external H_3PO_4 (62.5%) and are correct to ±0.1 ppm; a negative sign indicates a shift to higher field relative to the reference. Coupling constants are in Hz and are correct to ±3 Hz. [b] $^1H\{^{31}P\}$ INDOR measurements in CH_2Cl_2 referred to external H_3PO_4 (85%). [c] NO_3^- as counterion. [d] $\delta(PF_6) = -145.0$ (heptet, $^1J(P,F) = 712$ Hz). [e] In $CDCl_3$. [f] Present together with $[PtCl(P(tol)_3)_3]NO_3$ (ratio 1:1) in the solution obtained by mixing **20a** + $P(tol)_3$ + $AgNO_3$ (1:1:1).

the case of five-coordinate platinum(II)–phosphite complexes, that the ^{31}P signal of axial phosphites appears at higher field than that of equatorial phosphites. Moreover, Meier[40] has shown in the case of NiX_2L_3, that the relative positions of the ^{31}P signals (a doublet and a triplet) are the same whether L is trimethyl phosphite or trimethylphosphine. By analogy, the triplet should appear at higher field than that of the doublet for structure i and at lower field for structure ii. In fact the triplet is centered at −38.2 ppm and the doublet at −30.3 ppm. Thus structure ii is unlikely. Structure iii is also unlikely since the presence of an iodide ion in apical position should modify both $^1J(Pt,P)$ coupling constants with respect to those of $[PtI(PMe_3)_3]PF_6$. In fact, $^1J(Pt,P_1)$ is greater by ca. 750 Hz whereas $^1J(Pt,P_2)$ is only slightly affected (Table III). All structures, except v, should give rise to two IR bands corresponding to the Pt–I stretch. Since only one IR and Raman absorption is present in the ν(Pt–I) region (see Experimental Section), this leaves structure v as the proposed ideal structure for $PtI_2(PMe_3)_3$ in solution.

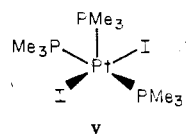

v

The addition of 2 equiv of L to PtX_2L_2 in dichloromethane solution gives rise to new observable species only in the case when L = PMe_3. The ^{31}P NMR spectrum of a mixture of $PtX_2(PMe_3)_2$ and PMe_3 (1:2) at −60 °C presents a singlet (with satellites due to Pt–P coupling). This singlet could result from a fast exchange between chemically nonequivalent phosphines; however, the $^{31}P\{^1H\}$ FT NMR spectrum in $CHClF_2$ down to −155 °C does not show any change either of the multiplicity or of the line width. Thus the species formed contain four coordinated phosphine ligands and are of C_{4v} symmetry. These "tetrakis" species should be formulated as $[PtX(PMe_3)_4]^+$ (X = Cl, Br, I) since their ^{31}P NMR spectra are different from that of $[Pt(PMe_3)_4](BF_4)_2$[36] and also since the chemical shift and the $^1J(Pt,P)$ coupling constant change when the nature of X is varied. Moreover, $[PtI(PMe_3)_4]^+$ is yellow whereas $[Pt(PMe_3)_4]^{2+}$ is colorless. No new species appear on adding a large excess of phosphine to PtX_2L_2; however, when the temperature is raised, a fast exchange of phosphine is observed in the case of $[PtCl(PMe_3)_4]^+$ and PMe_3 (vide infra).

2. Crystal Structure of $[PtCl(PMe_3)_3]Cl$. White needles of $[PtCl(PMe_3)_3]Cl$ were grown by slow evaporation of a mixture of *cis*-$PtCl_2(PMe_3)_2$ and PMe_3 (1:1.2) in dichloromethane–benzene under argon. All crystals were twinned; however, part of a single domaine was cleaved from a large needle. X-ray measurements were carried out with a Syntex $P2_1$ automatic four-circle diffractometer. The crystal data and the methods used for intensity collection, structure solution, and refinement are summarized in Table IV. The crystal form was accurately measured as before[41] and used to correct the

(40) Meier, P. Thèse de doctorat, Université de Lausanne, 1978.

(41) Pinkerton, A. A.; Carrupt, P. A.; Vogel, P.; Boschi, T.; Nguyen, Thuy Hai; Roulet, R. *Inorg. Chim. Acta* **1978**, *28*, 123.

Table IV. Summary of Crystal Data, Intensity Collection, and Refinement

formula	$[PtCl(PMe_3)_3]Cl$	radiation	Mo Kα, Nb filtered (λ = 0.710 69 Å)
mol wt	453.61	μ, cm^{-1}	91.9
dimens, mm	0.05 × 0.10 × 0.38	scan method	2θ–θ
cryst class	monoclinic	bkgd source	scan profile interpretation[46]
a, Å	29.468 (3)	$((\sin\theta)/\lambda)_{max}$	0.40
b, Å	11.032 (2)	data collected	$h, k > 0, \pm l$
c, Å	10.709 (1)	no. of unique reflctns	2252
β, deg	100.589 (8)	no. of reflctns $<3\sigma$	301
V, $Å^3$	3422.1 (7)	no. of obsns/no. of variables	16.6
Z	8		
d_{calcd}, g/cm^3	1.76	structure soln	Patterson and Fourier
F_{000}	1904	refinement method	full-matrix least squares
space group	$C2/c$	function minimized	$\Sigma w(\|F_o\| - \|F_c\|)^2$
systematic absences	hkl: $h + k = 2n + 1$	w	$1/\sigma^2$
	$h0l$: $l = 2n + 1$	R	0.029
		R_w	0.037
		goodness of fit	3.10

Table V. Atomic Coordinates and Thermal Parameters[a]

atom	x	y	z	U_{11}	U_{22}	U_{33}	U_{12}	U_{13}	U_{23}
Pt	0.14020 (1)	0.26755 (3)	0.06905 (3)	0.0207 (2)	0.0323 (2)	0.0247 (2)	−0.0016 (2)	−0.0009 (1)	0.0038 (2)
Cl(1)	0.21618 (9)	0.3473 (3)	0.1021 (2)	0.033 (1)	0.063 (2)	0.045 (2)	−0.017 (1)	0.000 (1)	0.010 (1)
Cl(2)	0.4184 (1)	0.3173 (3)	0.4766 (3)	0.048 (2)	0.065 (2)	0.058 (2)	−0.006 (2)	−0.004 (1)	−0.005 (1)
P(1)	0.06556 (8)	0.2154 (2)	0.0442 (2)	0.024 (1)	0.038 (2)	0.033 (1)	0.000 (1)	−0.001 (1)	−0.005 (1)
P(2)	0.17266 (8)	0.1233 (2)	0.2193 (2)	0.028 (1)	0.034 (1)	0.024 (1)	0.000 (1)	−0.003 (1)	0.002 (1)
P(3)	0.1298 (1)	0.3951 (2)	−0.1080 (2)	0.046 (2)	0.040 (2)	0.034 (1)	0.002 (1)	−0.002 (1)	0.011 (1)
C(11)	0.0286 (4)	0.348 (1)	0.048 (1)	0.032 (7)	0.046 (7)	0.095 (9)	0.008 (5)	0.007 (6)	−0.026 (6)
C(12)	0.0454 (4)	0.119 (1)	0.1604 (9)	0.036 (6)	0.094 (9)	0.037 (6)	−0.014 (6)	0.016 (5)	0.014 (6)
C(13)	0.0427 (3)	0.133 (1)	−0.1023 (8)	0.044 (7)	0.052 (7)	0.029 (5)	−0.002 (5)	−0.014 (5)	−0.016 (5)
C(21)	0.1420 (4)	0.0104 (9)	0.2935 (9)	0.052 (7)	0.055 (7)	0.039 (6)	−0.013 (6)	0.009 (5)	0.019 (5)
C(22)	0.2084 (4)	0.027 (1)	0.1345 (9)	0.056 (7)	0.058 (8)	0.032 (6)	0.022 (6)	0.007 (5)	−0.001 (5)
C(23)	0.2120 (4)	0.182 (1)	0.3583 (8)	0.060 (7)	0.050 (7)	0.023 (5)	−0.009 (6)	−0.017 (5)	−0.004 (5)
C(31)	0.1675 (4)	0.341 (1)	−0.2122 (9)	0.059 (8)	0.060 (8)	0.040 (6)	−0.001 (6)	0.016 (6)	0.000 (5)
C(32)	0.0751 (4)	0.414 (1)	−0.224 (1)	0.056 (9)	0.11 (1)	0.083 (9)	0.020 (8)	−0.023 (7)	0.056 (9)
C(33)	0.1476 (5)	0.551 (1)	−0.070 (1)	0.13 (1)	0.034 (7)	0.052 (7)	−0.005 (8)	0.000 (8)	0.012 (6)

[a] The temperature factor has the form e^{-T} where $T = 2\pi^2\Sigma h_i h_j U_{ij} a_i^* a_j^*$ for anisotropic atoms. The esd of the last significant digit is given in parentheses.

Table VI. Bond Lengths and Angles for $[PtCl(PMe_3)_3]Cl$[a]

Bond Lengths (Å)

Pt-P(1)	2.242 (3)	Pt-Cl(1)	2.371 (3)	P(1)-C(12)	1.819 (12)	P(2)-C(22)	1.845 (12)	P(3)-C(32)	1.855 (12)
Pt-P(2)	2.339 (2)	Pt···Cl(2)	5.251 (3)	P(1)-C(13)	1.832 (9)	P(2)-C(23)	1.829 (9)	P(3)-C(33)	1.826 (12)
Pt-P(3)	2.336 (3)	P(1)-C(11)	1.832 (11)	P(2)-C(21)	1.807 (11)	P(3)-C(31)	1.813 (12)		

Bond Angles (Deg)

P(1)-Pt-Cl(1)	172.81 (9)	Pt-P(1)-C(11)	111.4 (4)	C(11)-P(1)-C(12)	100.5 (5)
P(1)-Pt-P(2)	100.09 (9)	Pt-P(1)-C(12)	120.4 (3)	C(11)-P(1)-C(13)	106.9 (5)
P(1)-Pt-P(3)	94.49 (9)	Pt-P(1)-C(13)	115.4 (4)	C(12)-P(1)-C(13)	100.4 (5)
P(2)-Pt-Cl(1)	83.93 (9)	Pt-P(2)-C(21)	126.7 (3)	C(21)-P(2)-C(22)	101.5 (5)
P(2)-Pt-P(3)	160.83 (10)	Pt-P(2)-C(22)	104.5 (3)	C(21)-P(2)-C(23)	100.4 (5)
P(3)-Pt-Cl(1)	82.97 (9)	Pt-P(2)-C(23)	115.9 (3)	C(22)-P(2)-C(23)	105.6 (5)
Cl(1)-Pt···Cl(2)	130.55 (8)	Pt-P(3)-C(31)	107.4 (4)	C(31)-P(3)-C(32)	100.5 (5)
P(1)-Pt···Cl(2)	56.46 (7)	Pt-P(3)-C(32)	125.5 (5)	C(31)-P(3)-C(33)	105.2 (6)
P(2)-Pt···Cl(2)	60.42 (7)	Pt-P(3)-C(33)	113.5 (4)	C(32)-P(3)-C(33)	102.7 (6)
P(3)-Pt···Cl(2)	120.15 (7)				

Shortest Interatomic Distances (Nonbonded) (Å)

Pt···Pt	6.65 (1)	C···Cl(2)	3.68 (1)	Pt···C(22)	3.32 (1)	C···Cl(1)	3.32 (1)
P···Cl(2)	4.28 (1)	Cl(1)···Cl(2)	6.488 (4)	P···Cl(1)	3.118 (3)		

[a] The esd of the last significant digit is given in parentheses.

intensities for absorption. The computer programs used for the data reduction and structure analysis were taken from the X-RAY 72 program system.[42] Scattering factors for the neutral nonhydrogen atoms were taken from Cromer and Mann[43] and anomalous dispersion coefficients for Pt, P, and Cl from Cromer.[44] The structure was solved by Patterson and Fourier

Table VII. Best Least-Squares Plane for $PtCl_2(PMe_3)_3$

atoms defining mean plane	displacement of atoms from mean plane (Å)	eq of mean plane[a]
Pt	−0.055	$aX + bY + cZ - d = 0$
Cl(1)	−0.205	$a = 9.244$
P(1)	−0.163	$b = -7.569$
P(2)	0.206	$c = -7.527$
P(3)	0.216	$d = -1.194$

angle between Pt···Cl(2) line and normal to mean plane: 52.3°

[a] X, Y, and Z refer to the monoclinic coordinate system.

(42) Stewart, J. M.; Kundell, F. A.; Baldwin, J. C. X-RAY 72, version of June 1972, Technical Report TR-192 of the Computing Center, University of Maryland (as modified by D. Schwarzenbach).
(43) Cromer, D. T.; Mann, J. B. *Acta Crystallogr., Sect. A* **1968**, *24*, 321.
(44) Cromer, D. T. *Acta Crystallogr.* **1965**, *18*, 17.

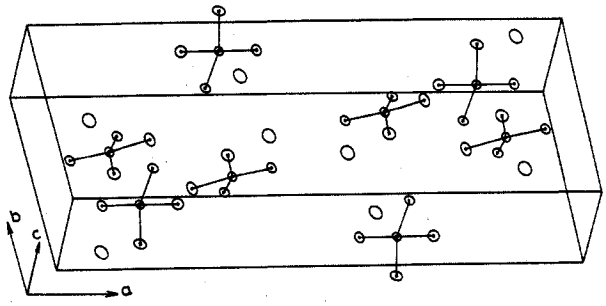

Figure 5. Contents of the unit cell of $[PtCl(PMe_3)_3]Cl$ (the methyl groups are omitted for clarity).

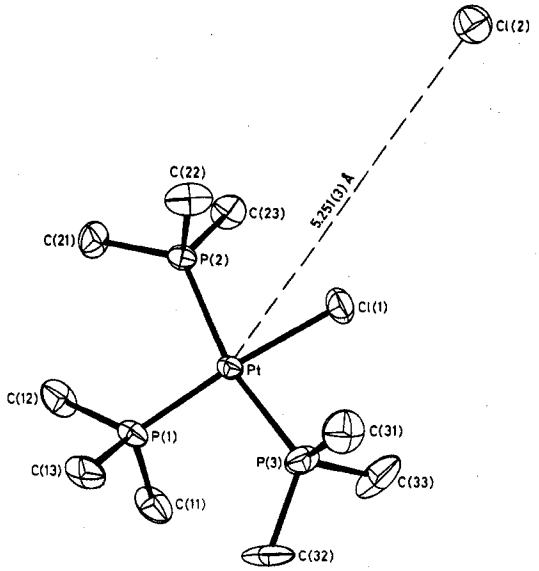

Figure 6. Perspective view of the $[PtCl(PMe_3)_3]^+$ cation and the nearest chloride ion.

methods and refined to a final residual $R = 0.029$. In the final cycles all atoms were allowed to vibrate anisotropically. Hydrogen atoms were not included in the model. The final positional and thermal parameters are listed in Table V. Calculated bond lengths and angles are reported in Table VI, and the equation of the best least-squares plane is given in Table VII. Views of the unit cell and of the cationic complex prepared by the program ORTEP[45] are given in Figures 5 and 6, respectively.

In the solid state $[PtCl(PMe_3)_3]Cl$ has to be considered as an ionic four-coordinate compound and not a molecular five-coordinated complex. Indeed, the four atoms P(1), P(2), P(3), and Cl(1) lie approximately in a plane at bonding distances from the platinum atom, whereas Cl(2) is at a distance of 5.251 (3) Å from the nearest platinum atom. This distance is much greater than the sum of the van der Waals radii of Pt and Cl.[47] Moreover Cl(2) is not located at an axial position corresponding to the fifth coordination site of a hypothetical tetragonal pyramid. Indeed, the line Pt···Cl(2) makes an angle of 52° with the normal to the least-squares mean plane defined by Pt, P(1), P(2), P(3), and Cl(1). The complex is tetrahedrally distorted; this distortion is however of the same order of magnitude as that observed by Ibers[48] in the "square-planar"

Chart I

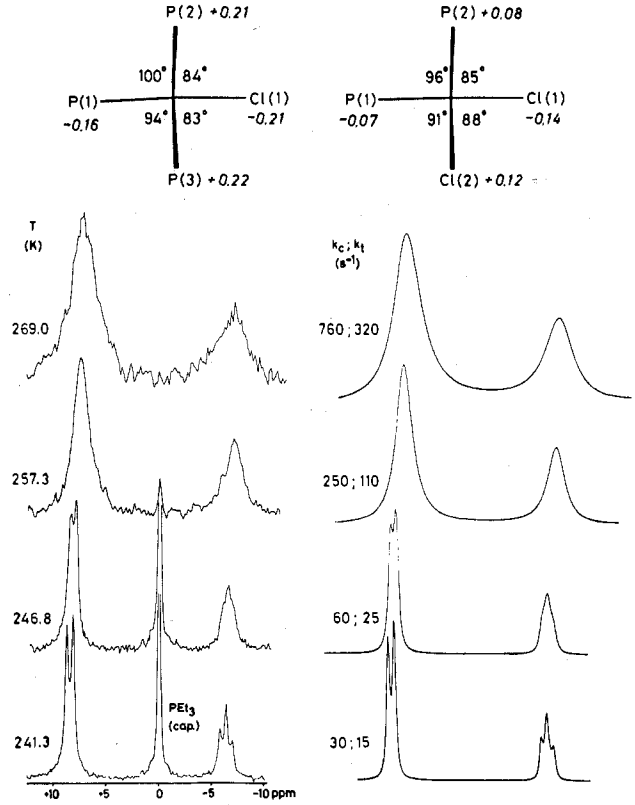

Figure 7. Experimental and calculated $^{31}P\{^1H\}$ FT NMR spectra for the intermolecular exchange of L in $[PtClL_3]Cl$ (L = PMe_3) as a function of temperature in CD_2Cl_2–CH_2Cl_2 (1:2) ([Pt] = 6×10^{-2} M).

complex *cis*-$PtCl_2(PMe_3)_2$ (Chart I; the deviations in Å of atoms from the mean plane are indicated in italics). The nonplanarity is essentially due to steric effects. The cone angle of PMe_3 is important,[49] and the resulting crowding in the region occupied by the van der Waals spheres of the methyl groups repels atoms P(2) and P(3) in the direction of Cl(1). Abnormally short interatomic contacts result from this, e.g., a distance C(23)···Cl(1) of 3.32 (1) Å which is shorter than the sum of the van der Waals radii of a methyl group (2.0 Å) and a chlorine atom (1.8 Å)[48] and a distance Pt···C(22) of 3.32 (1) Å. The distance Pt–Cl (1) of 2.371 (3) Å is in agreement with the Pt–Cl distance of 2.376 (8) Å found in *cis*-$PtCl_2(PMe_3)_2$ for a chlorine atom trans to phosphorus and is significantly longer than the Pt–Cl distance in *trans*-$PtCl_2(PEt_3)_2$ (2.294 (9) Å).[50] There is similarly a significative difference (0.096 (4) Å) between the distance Pt–P(1) (2.242 (3) Å) and the weighted average of Pt–P(2) and Pt–P(3) (2.338 (2) Å). These differences are due to the greater trans influence of phosphorus than of chlorine, which may also explain the difference between the observed coupling constants $^1J(Pt,P_1)$ and $^1J(Pt,P_2)$ (Table III).

3. Dynamic Processes Involving $[PClL_3]^+$, $[PtClL_4]^+$, and PtI_2L_3 (L = PMe_3). The $^{31}P\{^1H\}$ FT NMR spectrum of $[PtCl(PMe_3)_3]Cl$ in dichloromethane is temperature dependent and indicates that a fast exchange of phosphine takes place at room temperature. This process is intermolecular as shown by the following evidence: (i) On addition of a trace of $Pt_2Cl_4(PMe_3)_2$[51] to a solution of $[PtCl(PMe_3)_3]Cl$ in dichloromethane, the phosphine exchange is now blocked at room

(45) Johnson, C. K. Report ORNL-3794; Oak Ridge National Laboratory: Oak Ridge, Tenn., 1971.
(46) (a) Blessing, H.; Coppens, P.; Becker, P. *J. Appl. Crystallogr.* **1972**, *7*, 488. (b) Schwarzenbach, D. TWOTHLEH, a Syntex $P2_1$ data collection program including scan profile interpretation; see Abstracts, Fourth European Crystallographic Meeting, 1977; p 134.
(47) Pauling, L. "Nature of the Chemical Bond", 3rd ed.; Cornell University Press: Ithaca, N.Y., 1960; p 246 and ref 50.
(48) Messmer, G. G.; Amma, E. L.; Ibers, J. A. *Inorg. Chem.* **1967**, *6*, 725.
(49) Tolman, C. A. *J. Am. Chem. Soc.* **1970**, *92*, 2956.
(50) Messmer, G. G.; Amma, E. L. *Inorg. Chem.* **1966**, *5*, 1775.
(51) Goodfellow, R. J.; Venanzi, L. M. *J. Chem. Soc.* **1965**, 7533.

temperature. This is due to reaction 6 removing free PMe_3

$$[PtCl(PMe_3)_3]Cl \rightleftarrows cis\text{-}PtCl_2(PMe_3)_2 + PMe_3 \quad K_5 \ll 1 \tag{5}$$

$$Pt_2Cl_4(PMe_3)_2 + 2PMe_3 \rightleftarrows 2cis\text{-}PtCl_2(PMe_3)_2 \quad K_6 \tag{6}$$

formed in small amounts according to equilibrium 5. (ii) The exchange process takes place at the same rate in a solution of *cis*-$PtCl_2(PMe_3)_2$ + PMe_3 (1:1) of the same Pt(II) concentration. A similar exchange takes place with $[PtCl(PMe_3)_3]ClO_4$, and in all cases loss of ^{195}Pt–^{31}P coupling is observed. (iii) The spectrum of a 6×10^{-2} M solution of $[PtCl(PMe_3)_3]Cl$ in CD_2Cl_2–CH_2Cl_2 (1:2) was taken at various temperatures corresponding to the slow-exchange domain (the low boiling point of the solvent prevented measurements at higher temperatures). The spectra were simulated by the program EXCHNG[52] (Figure 7) for an intermolecular exchange with two rate constants.

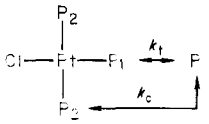

It proved impossible to fit the observed and calculated spectra if $k_c = k_t$; i.e., two parameters are indeed necessary. The residence times of the phosphine on a complexed site (τ_{compl}), on site P_1 (τ_{P_1}), and on site P_2 (τ_{P_2}) are related by the equations

$$1/\tau_{compl} = -d[PtClL_3]/dt[PtClL_3] = (k_2^c + k_2^t)[L] = k_c + k_t$$

$$1/\tau_{P_1} = k_t \qquad 1/\tau_{P_2} = \tfrac{1}{2}k_c$$

An exchange matrix for 16 sites was established by the method of Johnson and Moreland:[53] P_1 couples with P_2 and Pt giving a triplet of triplets (sites 1–9), P_2 couples with P_1 and Pt giving a triplet of doublets of double intensity (sites 10–15), and site 16 corresponds to the free phosphine. The nonzero matrix elements are

$$a_{ii} = -\tfrac{1}{2}k_c - k_t \quad (i = 1\text{–}9)$$
$$\text{or} \quad -\tfrac{1}{2}k_c - \tfrac{1}{2}k_t \quad (i = 10\text{–}15)$$

$$a_{i,i-1} = a_{i,i+1} = k_c/4 \quad (i = 2, 5, 8)$$

$$a_{j-1,j} = a_{j+1,j} = \tfrac{1}{2}k_c \quad (j = 2, 5, 8)$$

$$a_{i,i+1} = a_{i+1,i} = -\tfrac{1}{2}k_t \quad (i = 10, 12, 14)$$

$$a_{i,16} = k_t \quad (i = 1\text{–}9) \quad \text{or} \quad \tfrac{1}{2}k_c \quad (i = 10\text{–}15)$$

$$a_{16,j} = p_j k_t/p_{16} \quad (j = 1\text{–}9)$$
$$\text{or} \quad p_j k_c/2p_{16} \quad (j = 10\text{–}15)$$

$$a_{16,16} = -\sum_{i=1}^{9} p_i k_t/p_{16} - \tfrac{1}{2}\sum_{i=10}^{15} p_i k_c/p_{16}$$

where p_i is the population of site i. The population of the free phosphine was arbitrarily fixed at 0.001, and the calculated values of k_c and k_t reported in Table VIII did not vary significantly when p_{16} was varied by a factor of 10^2. The rate dependence on $[PMe_3]$ could not be obtained since $[PtCl(PMe_3)_4]^+$ appears in solution on addition of PMe_3 to $[PtCl(PMe_3)_3]^+$.

The rate-determining step for the exchange of phosphine is probably the dissociation of PMe_3 from a C_{4v} species formed by addition of PMe_3 to $[PtCl(PMe_3)_3]^+$. This is in agreement with the positive entropy of activation. Further evidence is presented by the observation of the square-pyramidal $[PtCl(PMe_3)_4]^+$ as a stable species in solutions of $[PtCl(PMe_3)_3]^+$ containing an excess of PMe_3. In the case of a C_{4v} complex, the probability of dissociation of a phosphine previously in a cis position to Cl should be twice that of a phosphine previously in a trans position to Cl giving a statistical ratio k_c/k_t of 2. Effectively, $k_c/k_t = 2.3 \pm 0.2$ over the temperature range studied (ΔT = 69 °C). This implies that the activation parameters related to k_c and k_t must be equal, as indeed observed (Table VIII). Thus, the two processes, although distinct from the NMR point of view, correspond in fact to a single chemical process, i.e., the equilibrium (7) where $^3/_4(k_2^c + k_2^t) = k_2 = K_7k_1$. Direct evidence for the process related to k_1 is provided as follows.

$$[PtCl(PMe_3)_3]^+ + PMe_3 \underset{k_1}{\overset{k_2}{\rightleftarrows}} [PtCl(PMe_3)_4]^+ \quad K_7 \gg 1 \tag{7}$$

The $^{31}P\{^1H\}$ FT NMR spectrum of a solution of $[PtCl(PMe_3)_4]^+$ containing an excess of PMe_3 presents a singlet (with satellites due to Pt–P coupling) at low temperature. When the temperature is raised, loss of Pt–P coupling and coalescence of the signals of free and bonded phosphine are observed, indicating an intermolecular exchange process. Variable-temperature spectra were taken by keeping the

Table VIII. Activation Parameters for the Phosphine-Exchange Process Involving $[PtCl(PMe_3)_3]^+$ and $PtI_2(PMe_3)_3$ in CD_2Cl_2

k_{300}, s^{-1}	ΔG^*_{300}, kcal/mol	ΔH^*,[c] kcal/mol	ΔS^*, eu
	$[PtCl(PMe_3)_3]Cl$[a]		
k_c = 14800	11.8 ± 0.2	14.6 ± 0.7[d]	9 ± 3
k_t = 6325	12.3 ± 0.2	14.6 ± 0.7[d]	8 ± 3
	$PtI_2(PMe_3)_3$[b]		
k_c = 990 ± 10	13.5 ± 0.1	13.8 ± 0.3[d]	1 ± 1
k_t = 442 ± 7	13.9 ± 0.1	15.4 ± 0.4[d]	5 ± 2

[a] [Pt] = 6×10^{-2} M. Temperature range examined was 239–308 K; $k_c/k_t = 2.3 \pm 0.4$ for this temperature range. [b] [Pt] = 6×10^{-2} M. Temperature range examined was 286–306 K; $k_c/k_t = 2.3 \pm 0.3$ for this temperature range. [c] Calculated from $\ln(k/T) = \ln(k_B/h) + \Delta S^*/R - \Delta H^*/RT$. [d] Alignment coefficients are 0.997, 0.997, 0.999, and 0.999, respectively.

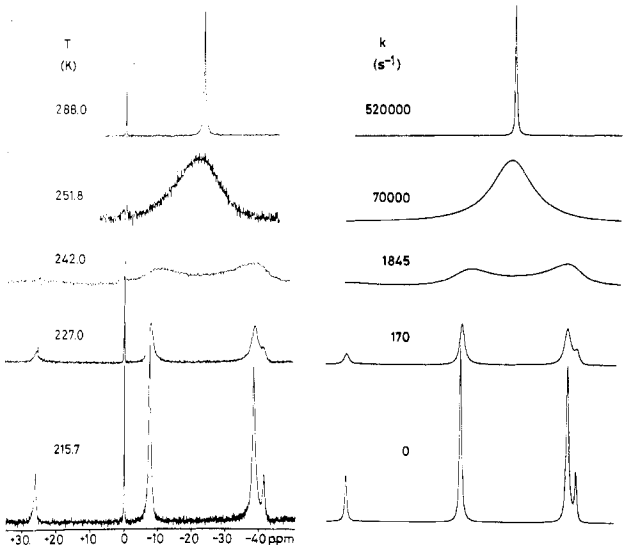

Figure 8. Experimental and calculated $^{31}P\{^1H\}$ FT NMR spectra for the intermolecular exchange between $[PtClL_4]^+$ and free L (L = PMe_3) (1:0.8) as a function of temperature in CD_2Cl_2–CH_2Cl_2 (1:2) ([Pt] = 6×10^{-2} M, PEt_3 as external reference).

(52) Christment, J.; Delpuech, J.-J.; Rubini, P. *Mol. Phys.* **1974**, *27*, 1163.
(53) Johnson, C. S.; Moreland, C. G. *J. Chem. Educ.* **1973**, *50*, 477.

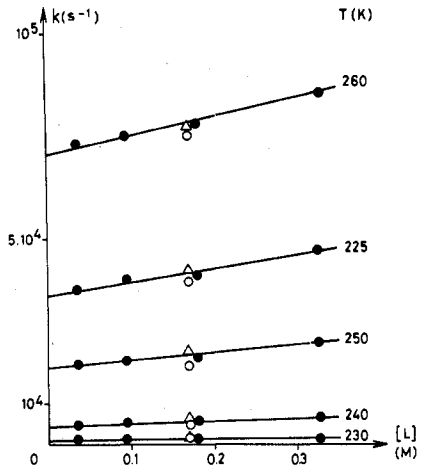

Figure 9. k vs. [L] for the exchange between $[PtClL_4]^+$ and free L (L = PMe_3) in CD_2Cl_2–CH_2Cl_2 (1:2) ([Pt] = 6×10^{-2} M): ●, no added Cl^-; △, $[Cl^-] = 1.2 \times 10^{-2}$ M; ○, $[Cl^-] = 3.0 \times 10^{-2}$ M.

Table IX. Activation Parameters for the Exchange of the $[PtCl(PMe_3)_4]^+$ Ion and PMe_3 in CD_2Cl_2

k_{250}	ΔG^*_{250}, kcal/mol	ΔH^*, kcal/mol	ΔS^*, eu
$k_1 = 18300\ s^{-1}$	9.7 ± 0.1	17 ± 1[a]	29 ± 2
$k_2 = 195\ M^{-1}\ s^{-1}$	12.0 ± 0.1	13 ± 1[b]	2 ± 3

[a] Temperature range examined is $225 < T < 265$ K; alignment coefficient of $\ln(KT^{-1})$ vs. T^{-1} is $bb' = 0.999$. [b] $bb' = 0.998$.

concentration of $[PtCl(PMe_3)_4]^+$ constant and by varying the concentration of free PMe_3 (Figure 8). These spectra were then simulated by the program EXCHNG by using an exchange matrix for four sites. Three sites were assigned to the triplet of $[PtClL_4]^+$ and were allowed to exchange with the fourth site (free L). The residence time on a complexed site (τ_{compl}) is then related to the observed rate constant k_{obsd} by the equation

$$1/\tau_{compl} = -d[PtClL_4]/dt[PtClL_4] = 4k_{obsd}$$

The rate dependence on the concentration of added phosphine (Figure 9) leads to the observed rate law

$$k = 4k_{obsd} = k_1 + k_3[PMe_3] \quad (8)$$

The activation parameters are reported in Table IX. The exchange pathway related to k_1 is clearly the dissociation of one phosphine from $[PtCl(PMe_3)_4]^+$ (eq 7). This is in agreement with the positive entropy of activation. Since the thermodynamic ΔS of equilibrium 7 must be smaller than zero, the entropy of activation for the backward reaction must be greater than that for the forward reaction. This is in agreement with $\Delta S^*_{k_1} = 29 \pm 2$ and $\Delta S^*_{k_2} = 9 \pm 3$ eu. The exchange pathway related to k_3 may correspond to the usual second-order pathway found in substitution reactions of Pt(II) complexes. We found that addition of $[AsPh_4]Cl$ to a solution of $[PtCl(PMe_3)_4]^+$ and PMe_3 does not affect the rate significantly (Figure 9). However, this does not necessarily imply a 20-electron transition state for the process related to k_3 since k_1 is much greater than $k_3[PMe_3]$ in eq 8.

The $^{31}P\{^1H\}$ FT NMR spectrum of $PtI_2(PMe_3)_3$ is also temperature dependent and indicates that a fast exchange of phosphine takes place at room temperature. This process is also intermolecular since the addition of a trace of $Pt_2I_4(PMe_3)_2$ to a solution of $PtI_2(PMe_3)_3$ in dichloromethane blocks the phosphine exchange at room temperature. The spectrum of a 6×10^{-2} M solution of $PtI_2(PMe_3)_3$ in CD_2Cl_2–CH_2Cl_2 (1:2) was taken at various temperatures corresponding to the slow-exchange domain. The spectrum was simulated for an intermolecular exchange with two rate constants k_c and k_t (vide supra), and the activation parameters are reported in Table VIII. As in the case of the $[PtCl(PMe_3)_3]^+$ ion, the ratio k_c/k_t is close to 2. Thus the phosphine exchange is due to a single chemical process, i.e., the equilibrium (9).

$$PtI_2(PMe_3)_3 + PMe_3 \underset{k_1}{\overset{k_2}{\rightleftharpoons}} [PtI(PMe_3)_4]^+ + I^- \quad K_9 \gg 1 \quad (9)$$

4. *cis*- ⇄ *trans*-$PtCl_2L_2$ Isomerization Mechanism in Dichloromethane Solution. In dichloromethane, the phosphine-catalyzed isomerization equilibrium (eq 10) favors the cis

$$trans\text{-}PtCl_2L_2 \underset{k_{-1}}{\overset{k_1}{\rightleftharpoons}} cis\text{-}PtCl_2L_2 \quad K_{10} > 1 \quad (10)$$

isomer (Tables I and II) and the equilibrium constant K_{10} at 30 °C decreases with the ligand sequence $PMe_3 \gg PEt_3$ (9.0) ≈ P-*n*-Bu_3 (9.2) > $P(tol)_3$ (5.25). The rate of approach to equilibrium (starting with the trans isomer) was followed spectrophotometrically at 20 °C (see Experimental Section) for L = PEt_3 and $P(tol)_3$ but was too fast to measure by conventional techniques for L = PMe_3. As expected, the observed rate law $k_{obsd} = (k_1 + k_{-1})[L]$ is first order in L with $k_1 = 11.2 \pm 0.5$ and $3.2 \pm 0.1\ M^{-1}\ s^{-1}$ and $k_{-1} = 1.2 \pm 0.1$ and $0.6 \pm 0.1\ M^{-1}\ s^{-1}$ for PEt_3 and $P(tol)_3$, respectively. The isomerization must go through one or several intermediates (or transition states) containing three bonded phosphines, and the double displacement mechanism (a) (see Introduction) implies that the intermediate is $[PtClL_3]^+$. Indeed, we have found that $[PtClL_3]^+$ is an observable species in mixtures of $PtCl_2L_2$ and L (Tables I and II). The measured equilibrium constant K_{11} at 30 °C for eq 11 decreases in the order L =

$$trans\text{-}PtCl_2L_2 + L \rightleftarrows [PtClL_3]^+ + Cl^- \quad K_{11} \quad (11)$$

$PMe_3 \gg PEt_3$ (0.53) > $P(tol)_3$ (0.087), and the equilibrium constant K_{12} for reaction 12 also decreases in the same manner,

$$cis\text{-}PtCl_2L_2 + L \rightleftarrows [PtClL_3]^+ + Cl^- \quad K_{12} \quad (12)$$

$PMe_3 \gg PEt_3$ (0.039) > $P(tol)_3$ (0.016). The trans effect of a phosphine being greater than that of Cl^-, the displacement of Cl by L from *trans*-$PtCl_2L_2$ must be slower than from *cis*-$PtCl_2L_2$. Likewise the displacement of L trans to Cl in $[PtClL_3]^+$ by Cl^- must be slower than that of L trans to L. This means that the rate-determining step for the isomerization is given by eq 11. An argument that has been used against the double displacement mechanism[7,15] is the inability of Cl^- to displace L from $[PtClL_3]^+$. This is in fact not so, at least in dichloromethane, as shown in Figure 10. Indeed, the $^{31}P\{^1H\}$ FT NMR spectrum of a solution of $[PtCl(P\text{-}n\text{-}Bu_3)_3]ClO_4$ shows the appearance of *cis*-$PtCl_2(P\text{-}n\text{-}Bu_3)_2$ when 1 equiv of $[AsPh_4]Cl$ is added. If the double displacement is operative, reaction 12 must be a fast process compared to cis–trans equilibration; i.e., addition of Cl^- to $[PtClL_3]^+$ must yield initially a higher proportion of *cis*-$PtCl_2L_2$ than that corresponding to the cis–trans isomerization equilibrium. This cannot be proved in the case L = P-*n*-Bu_3 where the various reactions are too fast to follow by NMR but is best shown in the case of $[Pt(CH_2CN)(PPh_3)_3]^+$ where the rate of approach to equilibrium allows the direct observation of both isomers by ^{31}P NMR.

cis-$PtCl(CH_2CN)(PPh_3)_2$[54] isomerizes slowly to the trans isomer. The reaction is catalyzed by free PPh_3, and the observed rate law is first order in PPh_3 with $k_1 = 2.3 \times 10^{-4}\ M^{-1}\ s^{-1}$ and $K_{10} = 0.25$ at 21 °C. The complex $[Pt(CH_2CN)(PPh_3)_3]Cl$ is not observed in solutions of the cis isomer con-

(54) Ros, R.; Renaud, J.; Roulet, R. *Helv. Chim. Acta* **1975**, *58*, 133.

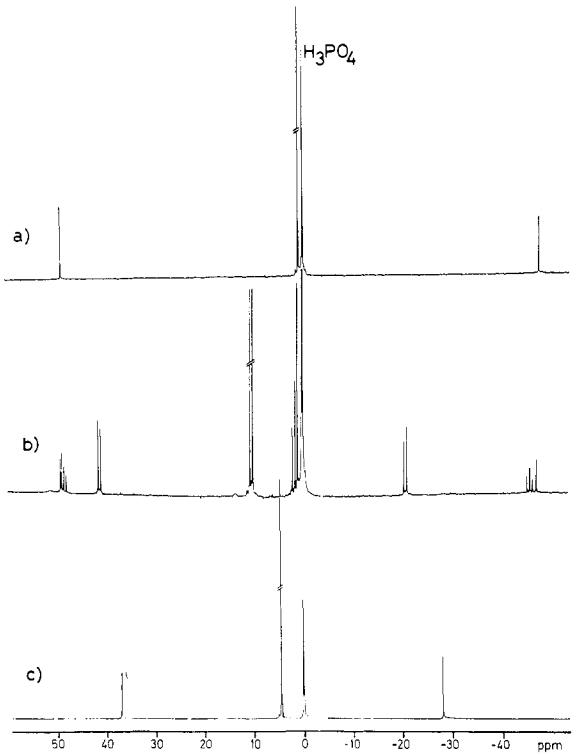

Figure 10. $^{31}P\{^1H\}$ FT NMR spectra in CD_2Cl_2 at 30 °C of (a) *cis*-$PtCl_2(P\text{-}n\text{-}Bu_3)_2$, (b) $[PtCl(P\text{-}n\text{-}Bu_3)_3]ClO_4$ and $[AsPh_4]Cl$ (1:1), and (c) *trans*-$PtCl_2(P\text{-}n\text{-}Bu_3)_2$.

Scheme I

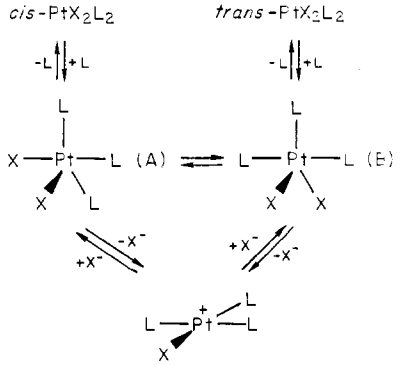

taining an excess of PPh_3; however, we were able to prepare and characterize $[Pt(CH_2CN)(PPh_3)_3]BF_4$.[54] Its $^{31}P\{^1H\}$ FT NMR spectrum shows an AX_2 pattern with a triplet (1:2:1) for the phosphorus atom P_1 trans to the alkyl group and a doublet twice an intense for the two phosphorus atoms P_2 trans to each other. The complex is stable in dichloromethane but addition of a stoichiometric amount of $[AsPh_4]Cl$ rapidly yields *cis*-$PtCl(CH_2CN)(PPh_3)_2$ (Figure 11). As this substitution liberates triphenylphosphine, the PPh_3-catalyzed isomerization then proceeds until the cis–trans equlibrium is reached.

Recently Louw[15] suggested an alternative mechanism (Scheme I) where isomerization proceeds via the pseudorotation A ⇄ B. Even though we did not observe species such as $PtCl_2L_3$ in solution, the equilibrium (13) must take place

$$[PtXL_3]^+ + X^- \rightleftarrows PtX_2L_3 \qquad (13)$$

in solution. Both species are definitively present in dichloromethane solution in the case X = I and L = PMe_3 as shown in Figure 12. The addition of increasing amounts of $[NBu_4]I$ to $[PtI(PMe_3)_3]PF_6$ gradually shifts the $^{31}P\{^1H\}$ FT NMR spectrum to that of $PtI_2(PMe_3)_3$, the equilibrium constant of reaction 13 being 340 ± 40 M^{-1} at −60 °C. It should however

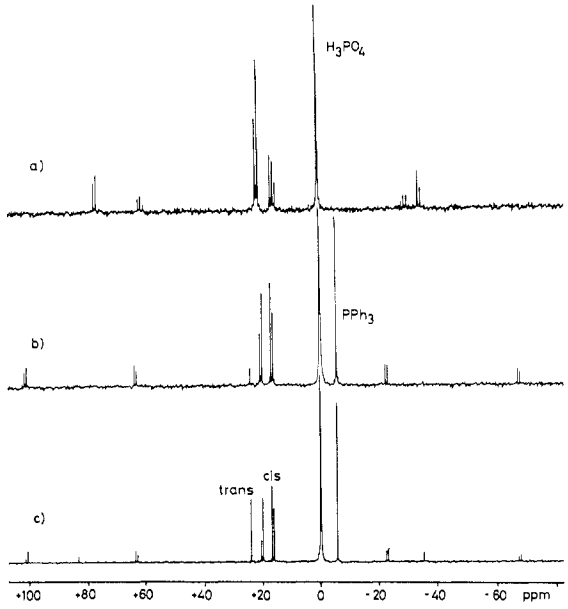

Figure 11. $^{31}P\{^1H\}$ FT NMR spectra in CD_2Cl_2 at 30 °C of (a) *cis*-$PtCl(CH_2CN)(PPh_3)_2$, (b) $[Pt(CH_2CN)(PPh_3)_3]ClO_4$ and $[AsPh_4]Cl$ (1:1) before cis ⇄ trans equilibration, and (c) same mixture at equilibrium.

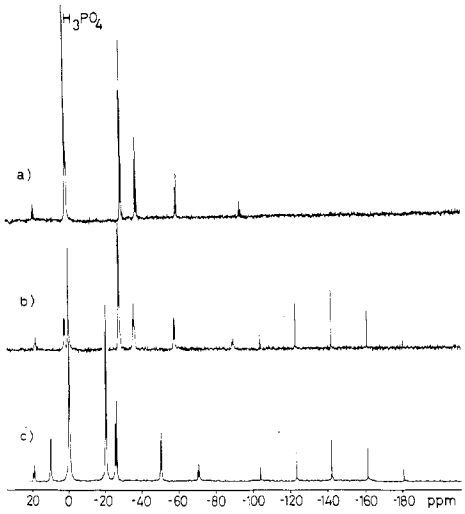

Figure 12. $^{31}P\{^1H\}$ FT NMR spectra in CD_2Cl_2 at −60 °C of (a) $PtI_2(PMe_3)_3$, (b) $[PtI(PMe_3)_3]PF_6$ and $[NBu_4]I$ (1:1), and (c) $[PtI(PMe_3)_3]PF_6$.

be noted that even though the exchange of phosphine is blocked at that temperature, a fast exchange of I^- ion must still be taking place between the four- and five-coordinate complexes since only one doublet and one triplet are observed (Figure 12b).

We have seen in the two limiting cases above that, for X = Cl where the observed species is $[PtCl(PMe_3)_3]^+$ and for X = I where $PtI_2(PMe_3)_3$ is now observed, no evidence for an intramolecular process of the type A ⇄ B could be found. The fastest process in each case is the intermolecular phosphine exchange through equilibriums 7 and 9, respectively. English, Meakin, and Jesson[34] have also shown that ligand dissociation from $[PtHL_4]^+$ (L = PEt_3) is rapid relative to the rate of intramolecular rearrangement of $[PtHL_4]^+$, and we find the same trend for $[PtCl(PMe_3)_4]^+$.

In conclusion, all the experimental results presented in this work are in agreement with the double-displacement mechanism (a) for cis–trans isomerization at platinum(II) in dichloromethane solution.

Experimental Section

Spectroscopic Measurements. Variable-temperature $^{31}P\{^1H\}$ FT NMR spectra were recorded at 36.43 MHz by using a Bruker HX-90 spectrometer equipped with a B-SW 3PM pulser, a B-SV 3B proton noise decoupler, a B-ST 100/700 temperature regulating unit, and a Nicolet BNC-12 data system. The spectra at −150 °C were obtained at 24.28 MHz by using a Bruker WP-60 spectrometer with multinuclei facilities. Field frequency stabilization was achieved on an internal ^2D signal at 21.14 kG and on an external ^{19}F signal at 14.09 kG. The temperature of the sample was measured before and after each spectrum by the method of substitution with a Pt resistance (100 Ω) coupled with a temperature measurement unit, Hewlett-Packard 2802-A.[55] As ^{31}P chemical shift reference at low temperature, we used pure PEt_3 in a capillary. The chemical shift of PEt_3 being temperature dependent (~0.03 ppm/K), we used the plot established by Meier[40] showing the chemical shift difference between PEt_3 and 62.5% H_3PO_4 (eutectic) as a function of temperature. At room temperature, we used 62.5% H_3PO_4 in a capillary. All chemical shifts are reported with respect to 62.5% H_3PO_4 with downfield shifts considered positive. The solid complexes, PPh_3 and $P(tol)_3$, were weighed in a nitrogen atmosphere glovebox (KSE) directly into 10-mm NMR tubes (Wilmad). Dichloromethane-d_2 (CEA, France) and chlorodifluoromethane (Freon 22, Du Pont) were deoxygenated in an all-glass-Teflon vacuum line by the freeze-pump-thaw technique. The solvents and volatile phosphines were vacuum distilled on the solid samples, and all tubes were sealed under vacuum and stored in liquid nitrogen.

UV spectra in dichloromethane were measured with a Beckman Acta V spectrophotometer, IR spectra with a Perkin-Elmer 577 spectrophotometer and a Bruker interferometer IFS-113C, and Raman spectra of powdered samples with a Spex Compact 1403 equipped with a Krypton laser (647 nm).

Isomerization Kinetic Measurements. (a) For $PtCl_2L_2$ (L = PEt_3, $P(tol)_3$), the approach to equilibrium was followed spectrophotometrically at 20 °C in the direction trans → cis. The evolution of the UV spectrum of a 3.26×10^{-5} M solution of *trans*-$PtCl_2(P(tol)_3)_2$ (λ_{max} = 287 nm with ϵ = 31 800 M^{-1} cm^{-1}) and excess $P(tol)_3$, in CH_2Cl_2 showed an isosbestic point at 272 nm. The concentration of $P(tol)_3$ was varied from 9×10^{-6} to 2.25×10^{-4} M, and the variation in absorbance was followed at 287 nm. The isomerization of *trans*-$PtCl_2(PEt_3)_2$ (λ_{max} = 247 nm, ϵ = 9720 M^{-1} cm^{-1}; 267 nm, 9820 M^{-1} cm^{-1}) was faster and followed at 267 nm ($[Pt]_0 = 9.7 \times 10^{-5}$ M; $[PEt_3]_0 = 2.84$ to 5.7×10^{-5} M). The observed rate constant k_{obsd} was obtained as the slope of $\ln [OD_0 - OD_\infty/(OD_t - OD_\infty)]$ vs. t. The second-order rate constants k_1 and k_{-1} (eq 10) were obtained from the slope of k_{obsd} vs. [L] and the value of K_{10}. In all cases, alignment coefficients were equal to or greater than 0.999. (b) For $PtCl(CH_2CN)L_2$ (L = PPh_3), the approach to equilibrium was followed by ^{31}P NMR at 21 °C in the direction cis → trans by integration of the undecoupled resonances of each isomer at various intervals of time and at equilibrium in the presence of different amounts of PPh_3 (for the trans isomer, $\delta(P)$ = 24.0; for the cis isomer, $\delta(P)$ = 20.0 and 16.8).

Preparation of Complexes. All reactions were carried out in an atmosphere of nitrogen. Solvents and volatile tertiary phosphines were transferred on vacuum lines. Trimethylphosphine[56] and the following complexes were prepared as reported in the literature: **1a,b**, **2a,b**, **3a,b**, **20a,b**;[19] **14a,b**;[57] **17a,b**;[25] **4**, **6**, **8**, **13**;[20] **15**, **18**, **21**;[35] *cis*- and *trans*-$PtCl(CH_2CN)(PH_3)_2$ and $[Pt(CH_2CN)(PPh_3)_3]BF_4$.[54] E. Manzer (Mikrolabor, ETH Zürich) carried out the microanalyses.

For $[PtCl(PMe_3)_3]Cl$ (**5**), 1 equiv of PMe_3 was transferred into a degassed solution of *cis*-$PtCl_2(PMe_3)_2$ (1 g) in acetone (40 mL) and the mixture stirred at room temperature for 10 min. A white powder precipitated on evaporating the solvent and was recrystallized from CH_2Cl_2–benzene; yield 85%. Anal. Calcd for $C_9H_{27}Cl_2P_3Pt$: C, 21.87; H, 5.51; P, 18.80. Found: C, 21.97; H, 5.64; P, 18.56. IR (Nujol): 300 cm^{-1} (ν(Pt–Cl)). UV (dichloromethane): 238 nm (ϵ 9700 M^{-1} cm^{-1}), 258 sh (2000). The same method was used for $[PtBr(PMe_3)_3]Br$ (**7**) and $PtI_2(PMe_3)_3$ (**9**), starting with **2a** and **3b**, respectively; yields 90 and 75%.

Compound **7** formed as white crystals. Anal. Calcd for $C_9H_{27}Br_2P_3Pt$: C, 18.54; H, 4.67; P, 15.93. Found: C, 18.20; H, 4.41; P, 15.68. IR (Nujol): 205 cm^{-1} (ν(Pt–Br)). UV (dichloromethane): 240 (sh) nm (ϵ 9000 M^{-1} cm^{-1}) (identical with spectrum of **6**).

Compound **9** appeared as air- and light-sensitive orange needles, mp 207–209 °C dec. Anal. Calcd for $C_9H_{27}I_2P_3Pt$: C, 15.96; H, 4.02; P, 13.72. Found: C, 16.23; H, 4.00; P, 13.81. IR: 148 cm^{-1} (ν(Pt–I)). Raman: 146 cm^{-1} (ν(Pt–I)). This IR band appears at 153 cm^{-1} for **8**. UV (dichloromethane): 248 nm (ϵ 25 580 M^{-1} cm^{-1}), 298 (16 670), 364 (5430). This UV spectrum is different from that of **8**: 249 nm (ϵ 31 280 M^{-1} cm^{-1}), 278 sh (15 390), 334 sh (5560).

Complexes **10**–**12**, **22**, and **23** were observed in solution only. Complexes **16** and **19** have the same spectral properties as those of **15** and **18**,[37] respectively.

The ^{35}Cl FT NMR spectrum of **4**[20] was recorded on a Bruker WP-60 spectrometer at 5.88 MHz with quadrature detection (time pulse 20 μs; spectrum with width 5000 Hz; 4096 points; ^2D lock). A line width of 4 Hz was found for its ClO_4^- signal, and a width of 3 Hz was found for $NaClO_4$ in D_2O.

Acknowledgment. We thank the Swiss National Science Foundation for financial support (Grant No 2.037-0.78) and Mrs. Michèle Dartiguenave (Université P. Sabatier, Laboratoire de Chimie de Coordination du CNRS, Toulouse, France) for a gift of trimethylphosphine.

Registry No. **1a**, 15630-86-1; **1b**, 21545-76-6; **2a**, 15703-02-3; **2b**, 23627-37-4; **3a**, 15703-03-4; **3b**, 21258-95-7; **4**, 72778-74-6; **5**, 72778-75-7; **6**, 72778-76-8; **7**, 72778-77-9; **8**, 72778-78-0; **9**, 72778-79-1; **10**, 72778-80-4; **11**, 72778-81-5; **12**, 72778-82-6; **13**, 21556-14-9; **14a**, 15692-07-6; **14b**, 13965-02-1; **15**, 22854-50-8; **16**, 72778-83-7; **17a**, 15390-92-8; **17b**, 15391-01-2; **18**, 72778-85-9; **19**, 72778-86-0; **20a**, 31173-67-8; **20b**, 31173-67-8; **21**, 72778-88-2; **22**, 72784-65-7; **23**, 72778-89-3; *cis*-$PtCl(CH_2CN)(PPh_3)_2$, 53702-17-3; *trans*-$PtCl(CH_2CN)(PPh_3)_2$, 42481-62-9; $[Pt(CH_2CN)(PPh_3)_3]BF_4$, 55641-50-4; $[Pt(CH_2CN)(PPh_3)_3]ClO_4$, 72778-90-6.

Supplementary Material Available: A listing of structure factor amplitudes (9 pages). Ordering information is given on any current masthead page.

(55) Ammann, C.; Meier, P.; Merbach, A. E., submitted for publication.

(56) Wolfsberger, W.; Schmidbaur, H. *Synth. Inorg. Met.-Org. Chem.* **1974**, *4*, 149.

(57) *Inorg. Synth.* **1970**, *12*, 27.